Output Tracking of Uncertain Nonminimum Phase Systems by Experience Replay

Linqi Ye, Qun Zong, *Member, IEEE*, and Bailing Tian, *Member, IEEE*

***Abstract*—The precision output tracking problem of multi-input–multi-output (MIMO) uncertain nonlinear nonminimum phase systems is investigated in this paper. The challenge lies in the difficulty in solving the ideal internal dynamics (IID), which is a bounded solution for the uncertain zero dynamics. First, the experience replay technique is applied to identify the uncertain parameters in the zero dynamics. It uses the recorded past data concurrently with current data which can greatly speed up the identification convergence. With the identified parameters, a novel approach called *optimal bounded inversion* is proposed to obtain the IID by solving a trajectory optimization problem using GPOPS-II. The boundedness of the IID is guaranteed by setting state constraints and the feasibility is achieved by minimizing the initial condition mismatch. Moreover, a piecewise IID updating scheme is adopted to reduce the computational burden. The benchmark nonminimum phase system, a vertical take-off and landing (VTOL) aircraft is used to validate the effectiveness of the proposed method.**

***Index Terms*—Experience replay, nonminimum phase, optimal bounded inversion, parameter identification, tracking control.**

I. Introduction

OUTPUT tracking of nonminimum phase systems is regarded as a challenging problem. Nonminimum phase systems are systems with unstable zero dynamics [1]. The stabilization of nonminimum phase systems can be achieved by designing an appropriate feedback controller, such as an output redefinition controller [2], a dynamic sliding mode controller [3], or a sampled-data output feedback controller [4]. However, the output tracking of nonminimum phase systems is much more difficult, which relies on the careful calculation of a feedforward signal that involves system inversion. It is well known that the traditional inversion-based tracking control method will result in an unbounded input when applied to nonminimum phase systems.

Manuscript received December 20, 2018; revised March 27, 2019; accepted May 10, 2019. Date of publication June 13, 2019; date of current version April 15, 2021. This work was supported by the National Natural Science Foundation of China under Grant 61673294 and Grant 61773278. This paper was recommended by Associate Editor M. Chen. *(Corresponding author: Bailing Tian.)*

L. Ye is with the School of Electrical and Information Engineering, Tianjin University, Tianjin 300072, China, and also with the Center for Artificial Intelligence and Robotics, Graduate School at Shenzhen, Tsinghua University, Shenzhen 518055, China (e-mail: yelinqi@tju.edu.cn).

Q. Zong and B. Tian are with the School of Electrical and Information Engineering, Tianjin University, Tianjin 300072, China (e-mail: zongqun@tju.edu.cn; bailing_tian@tju.edu.cn).

Color versions of one or more figures in this article are available at https://doi.org/10.1109/TSMC.2019.2919012.

Digital Object Identifier 10.1109/TSMC.2019.2919012

The key to achieving precision output tracking of nonminimum phase systems is to calculate a bounded solution of the zero dynamics, which is called the ideal internal dynamics (IID) [5], and then stabilize the internal states to the IID. Several methods have been proposed to obtain the IID. The first is the output regulation method [6], [7], which builds a regulation equation to calculate the state reference and input reference that can be transformed into the IID. The second is the stable system center method [8]–[10], where an estimator whose solution converges to the IID is constructed. However, both methods have the assumption of an exosystem to generate the output reference, which puts restrictions on the type of output references they can be applied to. The third is the stable inversion method [11]–[13], which sets up an important framework to calculate IID for arbitrary output references. The idea is to divide the zero dynamics into a stable part and an unstable part, and then the IID is obtained by integrating the stable part forward in time and the unstable part backward in time. The computing process of stable inversion involves a Picard-like iteration [11], [12]. Several alternatives are also available for the computation of stable inversion, such as the finite-difference method [14], the two-sided Laplace transformation method [15], and the method by solving a two-point boundary value problem [16], [17]. Implementation of stable inversion requires all the future information of the output reference. Preview-based stable inversion [18], [19] adopts a receding finite-time interval for the integration, making it possible to calculate the IID online. However, all the aforementioned methods can only be used when the zero dynamics are exactly known, that is, no system uncertainties. It is shown in [20] that when there are unknown disturbances in the zero dynamics, the best one can get is to keep the output tracking error within a certain bound. As for nonminimum phase systems with uncertain parameters, the output tracking problem has been studied in [21] and [22]. However, they focus on designing a robust feedback controller rather than solving the IID for the uncertain zero dynamics, which may sacrifice the tracking accuracy.

To sum up, IID is the key for precision output tracking of nonminimum phase systems. Several methods are available to calculate the IID but none of them can be used for uncertain zero dynamics. In this paper, we will focus on the IID calculation for nonminimum phase systems with uncertain parameters. This problem is quite challenging. On the one hand, it requires the identification of the true values of the uncertain parameters which will be used to predict the future information of the zero dynamics to get the IID. On

the other hand, the IID solver should be fast enough to work in real time with the identified parameters.

Motivated by [23] and [24], the recent developed experience replay technique is adopted to identify the uncertain parameters in the zero dynamics. Unlike the existing parameter identification algorithms, the recorded past data are used concurrently with current data for identification of the system parameters. By using this technique, the richness of the recorded data can guarantee convergence to the true values of the uncertain parameters. To achieve high-speed IID calculation, a novel method called *optimal bounded inversion* is proposed. It solves the IID from a trajectory optimization problem by using the powerful MATLAB software GPOPS-II [25]. In addition, a piecewise IID updating scheme is adopted to reduce the computational burden.

The main contributions of this paper are twofold. First, optimal bounded inversion is proposed for the IID calculation problem. It provides a new way to calculate the IID from the perspective of trajectory optimization and guarantees high efficiency as well as high accuracy. Second, the IID calculation for uncertain zero dynamics is solved for the first time by using the experience replay technique along with the proposed optimal bounded inversion method, which are very important for achieving precision output tracking for multi-input–multi-output (MIMO) nonlinear nonminimum phase systems with uncertain parameters.

The remainder of this paper is organized as follows. Section II gives the problem formulation. In Section III, the main results are presented. The application of the proposed method to a vertical take-off and landing (VTOL) aircraft is provided in Section IV. Then, simulation results are given in Section V. Finally, the conclusions are summarized in Section VI.

II. Problem Formulation

Consider an MIMO nonlinear nonminimum phase system

$$\boldsymbol{y}^{(r)} = \boldsymbol{F}_1(\boldsymbol{x}) + \boldsymbol{G}_1(\boldsymbol{x})\boldsymbol{u} \text{ (External Dynamics)} \tag{1}$$

$$\dot{\boldsymbol{\eta}} = \boldsymbol{F}_2(\boldsymbol{x}) + \boldsymbol{G}_2(\boldsymbol{x})\boldsymbol{u} \text{ (Internal Dynamics)} \tag{2}$$

where $\boldsymbol{y} = [y_1, y_2, \ldots, y_m]^T$ is the output vector with relative degree $\{r_1, r_2, \ldots, r_m\}$, and $\boldsymbol{u} = [u_1, u_2, \ldots, u_m]^T$ is the input vector. $\boldsymbol{y}^{(r)}$ is defined by $\boldsymbol{y}^{(r)} = [y_1^{(r_1)}, y_2^{(r_2)}, \ldots, y_m^{(r_m)}]^T$. $\boldsymbol{\eta}$ is the internal state vector and $\boldsymbol{x} = [\boldsymbol{\xi}, \boldsymbol{\eta}]^T$ is the state vector with $\boldsymbol{\xi} = [y_1, \dot{y}_1, \ldots, y_1^{(r_1-1)}, \ldots, y_m, \dot{y}_m, \ldots, y_m^{(r_m-1)}]^T$ being the external state vector.

When the outputs move along the given references $\boldsymbol{y}_r = [y_{1r}, y_{2r}, \ldots, y_{mr}]^T$, the external dynamics (1) turn into

$$\boldsymbol{y}_r^{(r)} = \boldsymbol{F}_1(\boldsymbol{\xi}_r, \boldsymbol{\eta}) + \boldsymbol{G}_1(\boldsymbol{\xi}_r, \boldsymbol{\eta})\boldsymbol{u} \tag{3}$$

where $\boldsymbol{\xi}_r = [y_{1r}, \dot{y}_{1r}, \ldots, y_{1r}^{(r_1-1)}, \ldots, y_{mr}, \dot{y}_{mr}, \ldots, y_{mr}^{(r_m-1)}]^T$ and $\boldsymbol{y}_r^{(r)} = [y_{1r}^{(r_1)}, y_{2r}^{(r_2)}, \ldots, y_{mr}^{(r_m)}]^T$. Then $\boldsymbol{u}$ is solved as

$$\boldsymbol{u} = \boldsymbol{G}_1(\boldsymbol{\xi}_r, \boldsymbol{\eta})^{-1}\Big(\boldsymbol{y}_r^{(r)} - \boldsymbol{F}_1(\boldsymbol{\xi}_r, \boldsymbol{\eta})\Big). \tag{4}$$

Substituting (4) into the internal dynamics (2) gives the zero dynamics

$$\dot{\boldsymbol{\eta}} = \boldsymbol{F}_2(\boldsymbol{\xi}_r, \boldsymbol{\eta}) + \boldsymbol{G}_2(\boldsymbol{\xi}_r, \boldsymbol{\eta})\boldsymbol{G}_1(\boldsymbol{\xi}_r, \boldsymbol{\eta})^{-1}\Big(\boldsymbol{y}_r^{(r)} - \boldsymbol{F}_1(\boldsymbol{\xi}_r, \boldsymbol{\eta})\Big). \tag{5}$$

For nonminimum phase systems, the zero dynamics (5) are unstable. To guarantee output tracking as well as internal dynamics stabilization, it is required to find a bounded solution $\boldsymbol{\eta}_r$ (i.e., the IID) for the zero dynamics corresponding to the output reference and then stabilize the zero dynamics to the IID. A most widely used tracking controller is

$$\boldsymbol{u} = \boldsymbol{u}_r + \boldsymbol{K}(\boldsymbol{x} - \boldsymbol{x}_r) \tag{6}$$

where

$$\boldsymbol{x}_r = \begin{bmatrix} \boldsymbol{\xi}_r \\ \boldsymbol{\eta}_r \end{bmatrix},\ \boldsymbol{u}_r = \boldsymbol{G}_1(\boldsymbol{\xi}_r, \boldsymbol{\eta}_r)^{-1}\Big(\boldsymbol{y}_r^{(r)} - \boldsymbol{F}_1(\boldsymbol{\xi}_r, \boldsymbol{\eta}_r)\Big). \tag{7}$$

In this controller, $\boldsymbol{u}_r$ is the input reference which is used as a feedforward and $\boldsymbol{K}(\boldsymbol{x} - \boldsymbol{x}_r)$ is a feedback with $\boldsymbol{K}$ being the feedback gain and $\boldsymbol{x}_r$ being the state reference. This control structure is quite regular in output regulation [6] and stable inversion [11]. Though this is a linear control law, it makes the system locally exponentially stable along the state trajectory. The precision output tracking ability depends on the exact solution of the feedforward signal and the state reference, which is the key for precision output tracking.

If the model is exactly known, then the zero dynamics are deterministic and the IID can be calculated by using stable inversion [11]. However, a more difficult case is considered in this paper with some uncertain parameters in the model, which leads to uncertain zero dynamics. We assume that the true values of some parameters are unknown in the model. What we know is that they are constants (of course bounded), and we may also know their nominal values. For example, the nominal values of the aerodynamic parameters for an aircraft are usually known, where their true values may deviate from the nominal values to a certain degree.

To state the problem, it is assumed that the system matrices $\boldsymbol{F}_1(\boldsymbol{x})$, $\boldsymbol{G}_1(\boldsymbol{x})$, $\boldsymbol{F}_2(\boldsymbol{x})$, and $\boldsymbol{G}_2(\boldsymbol{x})$ in (1) and (2) contain some uncertain parameters. For clarity and without loss of generality, take any one row from the dynamics (1) and (2), which can be expressed as

$$\dot{x}_i = f_i(\boldsymbol{x}) + \boldsymbol{g}_i(\boldsymbol{x})\boldsymbol{u} \tag{8}$$

where $\dot{x}_i$ represent any variable in $\boldsymbol{y}^{(r)}$ or $\dot{\boldsymbol{\eta}}$. Consider some linearly parameterized uncertainties (which are widely studied in adaptive control [26]–[28]) in $f_i(\boldsymbol{x})$ and $\boldsymbol{g}_i(\boldsymbol{x})$, and rewrite (8) as

$$\dot{x}_i = \boldsymbol{\vartheta}_i^T \boldsymbol{\Phi}_i(\boldsymbol{x}, \boldsymbol{u}) + \psi_i(\boldsymbol{x}, \boldsymbol{u}) \tag{9}$$

where $\psi_i(\boldsymbol{x}, \boldsymbol{u})$ is the certain part, and $\boldsymbol{\vartheta}_i^T \boldsymbol{\Phi}_i(\boldsymbol{x}, \boldsymbol{u})$ is the uncertain part with $\boldsymbol{\vartheta}_i \in \mathbb{R}^{n_i}$ being the constant uncertain parameter vector and $\boldsymbol{\Phi}_i(\boldsymbol{x}, \boldsymbol{u})$ being some known functions of system state and input.

The uncertainties in the model will be reflected in the zero dynamics (5). For convenience, we denote

$$\boldsymbol{\phi}(\boldsymbol{\eta}, t, \boldsymbol{\vartheta}) = \boldsymbol{F}_2(\boldsymbol{\xi}_r, \boldsymbol{\eta}) + \boldsymbol{G}_2(\boldsymbol{\xi}_r, \boldsymbol{\eta})\boldsymbol{G}_1(\boldsymbol{\xi}_r, \boldsymbol{\eta})^{-1} \times \Big(\boldsymbol{y}_r^{(r)} - \boldsymbol{F}_1(\boldsymbol{\xi}_r, \boldsymbol{\eta})\Big) \tag{10}$$

where $\boldsymbol{\vartheta}$ represents the uncertain parameters in the zero dynamics. Then the zero dynamics (5) can be rewritten as

$$\dot{\boldsymbol{\eta}} = \boldsymbol{\phi}(\boldsymbol{\eta}, t, \boldsymbol{\vartheta}). \tag{11}$$

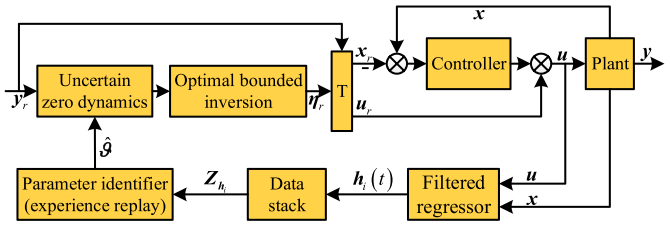

Fig. 1. Output tracking architecture for uncertain nonminimum phase systems.

Assumption 1: For each value of $\boldsymbol{\vartheta}$, $\boldsymbol{\phi}(\boldsymbol{\eta}, t, \boldsymbol{\vartheta})$ is continuous in t and $\boldsymbol{\eta}$, and Lipschitz continuous in $\boldsymbol{\eta}$.

Then the research objective is formulated as follows.

Research Objective: For the uncertain nonminimum phase system described by (1) and (2), in which each row may exist some uncertainties in the form described by (9), the aim of this paper is to solve the IID for the uncertain zero dynamics (11) and incorporate it into the tracking controller (6) to achieve precision output tracking for the output reference $\boldsymbol{y}_r$.

Remark 1: This paper focuses on the IID calculation for nonminimum phase systems with uncertain parameters, which is the key for precision output tracking. It is not our goal to present any new stabilization method. So we have adopted the standard tracking controller (6), which can guarantee the stability of the closed-loop system in first-order approximation. The feedback gain can be designed by using pole placement or linear quadratic regulator (LQR) technique. Other techniques for stabilization can be found in [2]–[4] (for uncertain nonminimum phase systems see [29], [30]).

III. Main Results

In this section, the main results are given to solve the problem presented in the previous section. First, parameter identification is derived by using the experience replay technique. Then, IID calculation is solved by using the proposed optimal bounded inversion method with the identified parameters. In the end, a piecewise IID updating scheme is introduced to reduce the computational burden.

The overall control architecture is given in Fig. 1.

In this control architecture, the system running data are stored in a data stack which provides information for the identifier to estimate the uncertain parameters. The identified parameters are applied to estimate the uncertain zero dynamics. Then the IID $\boldsymbol{\eta}_r$ is calculated online by applying optimal bounded inversion to the estimated zero dynamics. The state reference and input references $\boldsymbol{x}_r, \boldsymbol{u}_r$ are obtained using the transformation (7) and are embedded into the tracking controller (6) to achieve precision output tracking.

A. Parameter Identification by Experience Replay

Consider the uncertain system (9), the parameter identification task is to give an estimate for the uncertain parameter $\boldsymbol{\vartheta}_i$ and make the estimate converge to the true value asymptotically.

Lemma 1: The state of system (9) can be expressed as $x_i = \boldsymbol{\vartheta}_i^T \boldsymbol{h}_i + l_i$ with $\boldsymbol{h}_i$ and l_i being the outputs of the following filtered regressor:

$$\begin{aligned} \dot{\boldsymbol{h}}_i &= -a\boldsymbol{h}_i + \boldsymbol{\Phi}_i \\ \dot{l}_i &= -al_i + ax_i + \psi_i \end{aligned} \tag{12}$$

where $a > 0$ is a parameter to be designed.

Proof: Taking the derivative of $x_i = \boldsymbol{\vartheta}_i^T \boldsymbol{h}_i + l_i$ along (12)

$$\begin{aligned} \dot{x}_i &= \boldsymbol{\vartheta}_i^T \dot{\boldsymbol{h}} + \dot{l}_i \\ &= \boldsymbol{\vartheta}_i^T(-a\boldsymbol{h}_i + \boldsymbol{\Phi}_i) - al_i + ax_i + \psi_i \\ &= -a\left(\boldsymbol{\vartheta}_i^T \boldsymbol{h}_i + l_i - x_i\right) + \left(\boldsymbol{\vartheta}_i^T \boldsymbol{\Phi}_i + \psi_i\right) \\ &= \boldsymbol{\vartheta}_i^T \boldsymbol{\Phi}_i + \psi_i. \end{aligned} \tag{13}$$

It can be seen that (13) coincides with the expression (9). Therefore, the expression $x_i = \boldsymbol{\vartheta}_i^T \boldsymbol{h}_i + l_i$ is equivalent to the original expression (9). This completes the proof. ■

Denote the estimate for $\boldsymbol{\vartheta}_i$ as $\hat{\boldsymbol{\vartheta}}_i$, and the estimation error $\tilde{\boldsymbol{\vartheta}}_i = \boldsymbol{\vartheta}_i - \hat{\boldsymbol{\vartheta}}_i$. Then the estimate for x_i is $\hat{x}_i = \hat{\boldsymbol{\vartheta}}_i^T \boldsymbol{h}_i + l_i$, and the estimation error is $\tilde{x}_i = x_i - \hat{x}_i$.

The idea of experience replay is to use the recorded past data concurrently with current data to identify the uncertain parameters. Let

$$\boldsymbol{Z}_{\boldsymbol{h}_i} = [\boldsymbol{h}_i(t_1), \boldsymbol{h}_i(t_2), \ldots, \boldsymbol{h}_i(t_N)] \tag{14}$$

be the recorded data collected and stored in the data stack at the time instants $t_1, t_2, \ldots, t_N$, where t_1 is the current time, $t_2 \sim t_N$ are past times. The number of stored samples N in the data stack is fixed. The stored samples are collected and updated based on a data collection criterion (see later).

Define

$$\tilde{x}_i(t, t_j) = x_i(t_j) - \left[\hat{\boldsymbol{\vartheta}}_i^T(t)\boldsymbol{h}_i(t_j) + l_i(t_j)\right]. \tag{15}$$

Then the experience-replay-based updating law for the identifier is given by

$$\dot{\hat{\boldsymbol{\vartheta}}}_i(t) = \gamma_i \sum_{j=1}^{N} \boldsymbol{h}_i(t_j)\tilde{x}_i(t, t_j) \tag{16}$$

where γ_i is a positive learning rate.

Condition 1: The recorded data $\boldsymbol{Z}_{\boldsymbol{h}_i}$ has as many linearly independent elements as the dimension of the vector signal $\boldsymbol{h}_i$, that is, $\operatorname{rank}(\boldsymbol{Z}_{\boldsymbol{h}_i}) = \dim(\boldsymbol{h}_i) = n_i$.

Theorem 1: Given system (9) with uncertain parameters $\boldsymbol{\vartheta}_i$, by using the identification law (16), the parameter estimation error $\tilde{\boldsymbol{\vartheta}}_i = \boldsymbol{\vartheta}_i - \hat{\boldsymbol{\vartheta}}_i$ converges to zero exponentially if the recorded data (14) satisfy Condition 1.

Proof: Substituting $x_i = \boldsymbol{\vartheta}_i^T \boldsymbol{h}_i + l_i$ into (15) gives

$$\begin{aligned} \tilde{x}_i(t, t_j) &= \boldsymbol{\vartheta}_i^T \boldsymbol{h}_i(t_j) + l_i(t_j) - \left[\hat{\boldsymbol{\vartheta}}_i^T(t)\boldsymbol{h}_i(t_j) + l_i(t_j)\right] \\ &= \tilde{\boldsymbol{\vartheta}}_i^T(t)\boldsymbol{h}_i(t_j). \end{aligned} \tag{17}$$

Since $\tilde{\boldsymbol{\vartheta}}_i(t) = \boldsymbol{\vartheta}_i - \hat{\boldsymbol{\vartheta}}_i(t)$ and $\boldsymbol{\vartheta}_i$ is a constant, it follows that:

$$\dot{\tilde{\boldsymbol{\vartheta}}}_i(t) = -\dot{\hat{\boldsymbol{\vartheta}}}_i(t) = -\gamma_i \sum_{j=1}^{N} \boldsymbol{h}_i(t_j)\tilde{\boldsymbol{x}}_i(t, t_j). \tag{18}$$

Substituting (17) into (18) gives

$$\dot{\tilde{\boldsymbol{\vartheta}}}_i = -\gamma_i \sum_{j=1}^{N} \boldsymbol{h}_i(t_j)\tilde{\boldsymbol{\vartheta}}_i^T(t)\boldsymbol{h}_i(t_j). \tag{19}$$

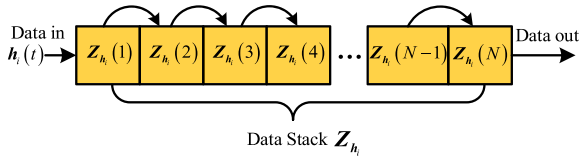

Fig. 2. Schematic of data collection.

Select the candidate Lyapunov function

$$V_i = \frac{1}{2\gamma_i}\tilde{\boldsymbol{\vartheta}}_i^T(t)\tilde{\boldsymbol{\vartheta}}_i(t). \tag{20}$$

Taking the derivative of V_i along (19) gives

$$\begin{aligned}\dot{V}_i &= \frac{1}{2\gamma_i}\left[\dot{\tilde{\boldsymbol{\vartheta}}}_i^T(t)\tilde{\boldsymbol{\vartheta}}_i(t) + \tilde{\boldsymbol{\vartheta}}_i^T(t)\dot{\tilde{\boldsymbol{\vartheta}}}_i(t)\right] \\ &= -\frac{1}{2}\left\{\left[\sum_{j=1}^{N}\boldsymbol{h}_i(t_j)\tilde{\boldsymbol{\vartheta}}_i^T(t)\boldsymbol{h}_i(t_j)\right]^T\tilde{\boldsymbol{\vartheta}}_i(t)\right. \\ &\qquad \left. + \tilde{\boldsymbol{\vartheta}}_i^T(t)\sum_{j=1}^{N}\boldsymbol{h}_i(t_j)\tilde{\boldsymbol{\vartheta}}_i^T(t)\boldsymbol{h}_i(t_j)\right\} \\ &= -\frac{1}{2}\left[\sum_{j=1}^{N}\boldsymbol{h}_i^T(t_j)\tilde{\boldsymbol{\vartheta}}_i(t)\boldsymbol{h}_i^T(t_j)\tilde{\boldsymbol{\vartheta}}_i(t)\right. \\ &\qquad \left. + \tilde{\boldsymbol{\vartheta}}_i^T(t)\sum_{j=1}^{N}\boldsymbol{h}_i(t_j)\tilde{\boldsymbol{\vartheta}}_i^T(t)\boldsymbol{h}_i(t_j)\right] \\ &= -\tilde{\boldsymbol{\vartheta}}_i^T(t)\left[\sum_{j=1}^{N}\boldsymbol{h}_i(t_j)\boldsymbol{h}_i^T(t_j)\right]\tilde{\boldsymbol{\vartheta}}_i(t) \\ &= -\tilde{\boldsymbol{\vartheta}}_i^T(t)\left(\boldsymbol{Z}_{\boldsymbol{h}_i}\boldsymbol{Z}_{\boldsymbol{h}_i}^T\right)\tilde{\boldsymbol{\vartheta}}_i(t). \end{aligned} \tag{21}$$

Therefore, if Condition 1 is satisfied, then $\boldsymbol{Z}_{\boldsymbol{h}_i}\boldsymbol{Z}_{\boldsymbol{h}_i}^T > 0$ holds and we have $\dot{V}_i < 0$. This indicates that $\tilde{\boldsymbol{\vartheta}}_i(t)$ converges to zero exponentially and completes the proof. ■

Remark 2: Condition 1 is less restrictive compared to the persistence of excitation (PE) condition [31] required in traditional identification law which only uses instantaneous data. By using the recorded data, it is possible to meet Condition 1 when the system states are exciting for a finite period. It is also possible to meet Condition 1 by recording data over a longer period without requiring special excitation.

To avoid collecting repeated data, the following criterion is proposed to manage the data collection.

Data Collection Criterion: Collect data at time t if the values of $\boldsymbol{h}_i(t)$ are sufficiently different from any data point stored in the data stack, that is, $\min_{k\in\{2,3,\ldots,N\}}\|\boldsymbol{h}_i(t) - \boldsymbol{Z}_{\boldsymbol{h}_i}(k)\| \geq \delta_{\text{th}}$, where $\boldsymbol{Z}_{\boldsymbol{h}_i}(k)$ denotes the kth column in the data stack (i.e., the kth data point) and $\delta_{\text{th}} > 0$ is the data collection threshold.

The data collection process is shown in Fig. 2. The number of stored data points in the data stack is fixed to N. Initial data in the stack are all set to zero. The first data point $\boldsymbol{Z}_{\boldsymbol{h}_i}(1)$ always keeps updating to the current data $\boldsymbol{h}_i(t)$. By "collecting data" we mean shifting the data points in the data stack by one position with the oldest data point $\boldsymbol{Z}_{\boldsymbol{h}_i}(N)$ being removed.

B. IID Calculation by Optimal Bounded Inversion

Consider the uncertain zero dynamics (11), since $\boldsymbol{\phi}(\boldsymbol{\eta}, t, \boldsymbol{\vartheta})$ depends on the uncertain parameters $\boldsymbol{\vartheta}$, by using the estimate $\hat{\boldsymbol{\vartheta}}$ to replace $\boldsymbol{\vartheta}$, it gives the estimate $\boldsymbol{\phi}(\boldsymbol{\eta}, t, \hat{\boldsymbol{\vartheta}})$, then the zero dynamics are estimated by

$$\dot{\boldsymbol{\eta}} = \boldsymbol{\phi}\left(\boldsymbol{\eta}, t, \hat{\boldsymbol{\vartheta}}\right). \tag{22}$$

This will be used for the IID calculation.

Denote the true IID [bounded solution for (11)] as $\boldsymbol{\eta}_r(t, \boldsymbol{\vartheta})$ and the calculated IID [bounded solution for (22)] as $\boldsymbol{\eta}_r(t, \hat{\boldsymbol{\vartheta}})$. Based on Assumption 1, and according to the ODE solution's continuous dependence on parameters [32], it follows that $\lim_{\|\boldsymbol{\vartheta}-\hat{\boldsymbol{\vartheta}}\|\to 0}\|\boldsymbol{\eta}_r(t, \boldsymbol{\vartheta}) - \boldsymbol{\eta}_r(t, \hat{\boldsymbol{\vartheta}})\| = 0$. Since $\hat{\boldsymbol{\vartheta}}$ will converge to $\boldsymbol{\vartheta}$, the calculated IID will also converge to the true IID asymptotically.

Now consider the IID calculation for (22). The task is to find a bounded solution $\boldsymbol{\eta}_r$ as the reference trajectories for the internal states. A typical method to calculate the IID is the stable inversion method [11], which linearizes the zero dynamics and divides it into a stable part and an unstable part, and then integrate the stable part forward in time and the unstable part backward in time with a Picard-like iteration. However, stable inversion involves some technical details which are hard to understand and put barriers for its implementation and programming. Since the core of IID is to find a state trajectory, it naturally reminds us of associating it with a trajectory optimization problem. First, the zero dynamics (22) can be treated as dynamic constraints. Second, to guarantee the boundedness, we can set constraints on the internal states. Third, to reduce the initial condition mismatch [12], we can take minimal initial condition mismatch as the optimization goal. In this way, the IID calculation problem is transformed into a standard trajectory optimization problem, which can be solved by the existing optimization software. Therefore, the only thing we need to do is to describe the problem in a standard form, while the technical details are segregated. Formally, we define the optimal bounded inversion problem as follows.

Optimal Bounded Inversion Problem: Determine the trajectory $\boldsymbol{\eta}_r(t)$ in the time interval $t \in [t_c, t_c + T_p]$ that minimizes the cost function

$$J = \left\|\boldsymbol{\eta}(t_c) - \boldsymbol{\eta}_r(t_c)\right\| \tag{23}$$

subject to the dynamic constraints

$$\dot{\boldsymbol{\eta}}_r = \boldsymbol{\phi}\left(\boldsymbol{\eta}_r, t, \hat{\boldsymbol{\vartheta}}\right) \tag{24}$$

and the state constraints

$$\boldsymbol{\eta}_{\min} \leq \boldsymbol{\eta}_r \leq \boldsymbol{\eta}_{\max} \tag{25}$$

where $[\boldsymbol{\eta}_{\min}, \boldsymbol{\eta}_{\max}]$ are the desired boundaries for the internal states. t_c is the IID updating instant, and T_p is the preview time. $\boldsymbol{\eta}(t_c)$ is the actual value of the internal state at the beginning of the current time interval while $\boldsymbol{\eta}_r(t_c)$ is the desired value. It is obvious that the boundedness of the IID is guaranteed by the state constraints (25). And the cost function (23) aims to minimize the initial condition mismatch of the internal states, thus it can reduce the initial tracking error as much as possible.

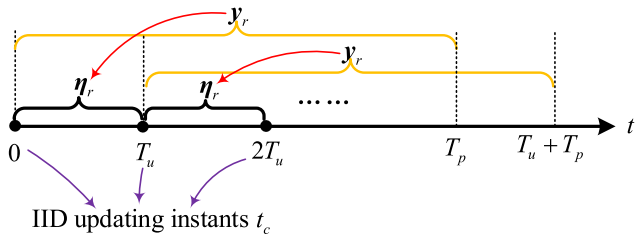

Fig. 3. Piecewise IID updating scheme.

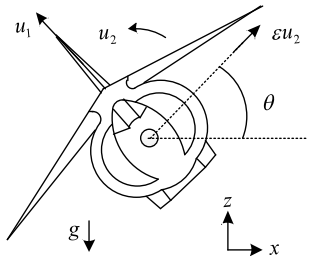

Fig. 4. Planar VTOL aircraft.

Remark 3: The complexity of the proposed trajectory optimization problem is relatively low. First, it is a single-phase trajectory optimization problem with simple state constraints. Second, the optimization problem is designed for the zero dynamics rather than the full model of the plant. So the order of the dynamic equations in the optimization problem is greatly reduced, which also reduces the complexity.

The trajectory optimization problem defined above can be easily solved by using GPOPS-II [25], which is a general purpose software for solving optimal control problems using variable-order adaptive orthogonal collocation methods together with sparse nonlinear programming. Compared to the stable inversion method, the proposed optimal bounded inversion method can minimize the initial condition mismatch so that the initial tracking error can be reduced. In addition, optimal bounded inversion takes advantage of the powerful optimization tool GPOPS-II, making it easy to implement and has high efficiency as well as high accuracy.

C. Piecewise IID Updating Scheme

Due to the model uncertainties, the IID needs to be updated repeatedly with the current identified parameters. However, there is no need to update the IID at each time step. Instead, it can be updated at a fixed frequency to reduce the computational burden. To this end, a piecewise IID updating scheme is proposed as shown in Fig. 3.

The IID is updated at the time instants $t_c = 0, \boldsymbol{T_u}, 2\boldsymbol{T_u}, \ldots$, where $\boldsymbol{T_u}$ is the updating period. At each updating instant t_c, the IID $\boldsymbol{\eta}_r$ is calculated by optimal bounded inversion with the preview information of the desired output in $t \in [t_c, t_c + T_p]$, where T_p is the preview time which is bigger than the updating period $\boldsymbol{T_u}$. Only the IID in the early period $t \in [t_c, t_c + \boldsymbol{T_u}]$ is used in the controller, and then at time $t_c + \boldsymbol{T_u}$ the IID is updated for the next time interval. This is the piecewise IID updating scheme. It can significantly reduce the computational burden and allows our method to be applied in real-time applications.

Remark 4: For the updating period $\boldsymbol{T_u}$, it should be small so that the calculated IID is based on the recent identified parameters. But if it is too small, the IID will update very frequently which will occupy a large amount of computing resources. Specifically, we fix $\boldsymbol{T_u} = 1$ s in the simulation. As for the preview time T_p, it should be much bigger than $\boldsymbol{T_u}$ (we select $T_p = 10$ s in the simulation). This is motivated by the fact that the preview information of the future desired output is important to calculate the current IID due to the noncausality of nonminimum phase systems [11], [12]. Another fact is that the effect of the far-future desired output on the current IID is small. Therefore, by adopting the preview information of the desired output in a finite-time window $[t_c, t_c + T_p]$ to compute the IID in $[t_c, t_c + \boldsymbol{T_u}]$, it is sufficient to guarantee the accuracy of the IID with a sufficiently large T_p. Please see [18] for more detail about the impact of the preview time.

IV. Application to VTOL Aircraft

In this section, the proposed method is applied to a benchmark nonminimum phase system, a planar VTOL aircraft as shown in Fig. 4.

A. VTOL Aircraft Model

Following [18], the dynamic equations of a VTOL aircraft are

$$\begin{aligned} \ddot{x} &= -u_1 \sin\theta + \varepsilon u_2 \cos\theta \\ \ddot{z} &= u_1 \cos\theta + \varepsilon u_2 \sin\theta - g \\ \ddot{\theta} &= \lambda u_2 \end{aligned} \tag{26}$$

where x and z are the horizontal and vertical positions of the aircraft mass center, respectively, θ is the roll angle, and $g = 1$ is the normalized gravitational acceleration. The inputs $u_1 = T/m$ and $u_2 = 2F\cos\alpha/m$ (T be the thrust, m be the mass, F be the RCS force, and α be the cathedral angle) represent the normalized thrust and the normalized rolling moment, respectively. Considering that the parameters ε and λ and the parameters contained in u_1 and u_2 may deviate from their nominal values, the model with uncertain parameters can be written as

$$\begin{aligned} \ddot{x} &= -\vartheta_1 u_1 \sin\theta + \vartheta_2 u_2 \cos\theta \\ \ddot{z} &= \vartheta_3 u_1 \cos\theta + \vartheta_4 u_2 \sin\theta - 1 \\ \ddot{\theta} &= \vartheta_5 u_2 \end{aligned} \tag{27}$$

where ϑ_1–ϑ_5 are the uncertain parameters. Their nominal values are taken as 1, which may deviate from their true values. The system outputs are x and z and the control objective is to let them track the references x_r and z_r.

B. Parameter Identification

Define $\dot{x} = v_x$, $\dot{z} = v_z$, and $\dot{\theta} = v_\theta$, then the uncertain VTOL aircraft model (27) can be written in the form

of (9) as

$$\begin{aligned}\dot{v}_x &= \boldsymbol{\vartheta}_x^T \boldsymbol{\Phi}_x \\ \dot{v}_z &= \boldsymbol{\vartheta}_z^T \boldsymbol{\Phi}_z + \psi_z \\ \dot{v}_\theta &= \boldsymbol{\vartheta}_\theta^T \boldsymbol{\Phi}_\theta \end{aligned} \tag{28}$$

where $\boldsymbol{\vartheta}_x = [\vartheta_1, \vartheta_2]^T$, $\boldsymbol{\vartheta}_z = [\vartheta_3, \vartheta_4]^T$, $\boldsymbol{\vartheta}_\theta = \vartheta_5$, and

$$\begin{aligned}\boldsymbol{\Phi}_x &= [-u_1 \sin\theta, u_2 \cos\theta]^T \\ \boldsymbol{\Phi}_z &= [u_1 \cos\theta, u_2 \sin\theta]^T, \ \ \psi_z = -1 \\ \boldsymbol{\Phi}_\theta &= u_2. \end{aligned} \tag{29}$$

According to Lemma 1, the states v_x, v_z, and v_θ can be represented by

$$v_x = \boldsymbol{\vartheta}_x^T \boldsymbol{h}_x + l_{\boldsymbol{x}}, \ \ v_z = \boldsymbol{\vartheta}_z^T \boldsymbol{h}_z + l_z, \ \ v_\theta = \boldsymbol{\vartheta}_\theta^T \boldsymbol{h}_\theta + l_\theta \tag{30}$$

with the following filtered regressor:

$$\begin{cases} \dot{\boldsymbol{h}}_x = -a\boldsymbol{h}_x + \boldsymbol{\Phi}_x, & \dot{l}_x = -al_x + av_x \\ \dot{\boldsymbol{h}}_z = -a\boldsymbol{h}_z + \boldsymbol{\Phi}_z, & \dot{l}_z = -al_z + av_z - 1 \\ \dot{\boldsymbol{h}}_\theta = -a\boldsymbol{h}_\theta + \boldsymbol{\Phi}_\theta, & \dot{l}_\theta = -al_\theta + av_\theta. \end{cases} \tag{31}$$

Then the updating law for the identifier is

$$\begin{aligned}\dot{\hat{\boldsymbol{\vartheta}}}_x &= \gamma_x \sum_{j=1}^{N} \boldsymbol{h}_x(t_j) \tilde{v}_x(t, t_j) \\ \dot{\hat{\boldsymbol{\vartheta}}}_z &= \gamma_z \sum_{j=1}^{N} \boldsymbol{h}_z(t_j) \tilde{v}_z(t, t_j) \\ \dot{\hat{\boldsymbol{\vartheta}}}_\theta &= \gamma_\theta \sum_{j=1}^{N} \boldsymbol{h}_\theta(t_j) \tilde{v}_\theta(t, t_j) \end{aligned} \tag{32}$$

where $\tilde{v}_{\boldsymbol{x}}(t, t_j)$, $\tilde{v}_z(t, t_j)$, and $\tilde{v}_\theta(t, t_j)$ are defined as (15).

C. IID Calculation

For the uncertain VTOL aircraft model (27), the zero dynamics are obtained as

$$\ddot{\theta} = \vartheta_5 \frac{\vartheta_1 \sin\theta + \vartheta_3 \ddot{x}_r \cos\theta + \vartheta_1 \ddot{z}_r \sin\theta}{\vartheta_2 \vartheta_3 \cos^2\theta + \vartheta_1 \vartheta_4 \sin^2\theta}. \tag{33}$$

Denote $\eta_1 = \theta, \eta_2 = \dot{\theta}$ and replace the uncertain parameters by their estimates, then the estimated zero dynamics are

$$\begin{bmatrix} \dot{\eta}_1 \\ \dot{\eta}_2 \end{bmatrix} = \begin{bmatrix} \eta_2 \\ \hat{\vartheta}_5 \frac{\hat{\vartheta}_1 \sin\eta_1 + \hat{\vartheta}_3 \ddot{x}_r \cos\eta_1 + \hat{\vartheta}_1 \ddot{z}_r \sin\eta_1}{\hat{\vartheta}_2 \hat{\vartheta}_3 \cos^2\eta_1 + \hat{\vartheta}_1 \hat{\vartheta}_4 \sin^2\eta_1} \end{bmatrix}. \tag{34}$$

This is used for IID calculation by using the proposed optimal bounded inversion method. Then the state reference and input reference $\boldsymbol{x}_r, \boldsymbol{u}_r$ can be obtained from the IID, and the tracking controller is given by (6) with $\boldsymbol{x} = [x, \dot{x}, z, \dot{z}, \theta, \dot{\theta}]^T$.

V. Simulations

A. Simulation Results

To verify the effectiveness of the proposed method, the true values of the uncertain parameters are assumed to be $\vartheta_1 = 0.8$, $\vartheta_2 = 1.2$, $\vartheta_3 = 1.2$, $\vartheta_4 = 0.8$, and $\vartheta_5 = 1.2$, which differ from their nominal value 1. The output references are given as $x_r = \sin t$ and $z_r = \cos t$.

TABLE I
Controller Parameters

Parameter meaning	Parameter value
Filtered regressor gain	$a = 1$
Identifier learning rate	$\gamma_x = \gamma_z = \gamma_\theta = 1$
IID preview time	$T_p = 10\,s$
IID updating period	$T_u = 1\,s$
Feedback control gain	$\boldsymbol{K} = \begin{bmatrix} 0 & 0 & -0.45 & -0.96 & 0 & 0 \\ 0.45 & 1.71 & 0 & 0 & -3.26 & -4.09 \end{bmatrix}$
Data collection threshold	$\delta_{th} = 0.02$
Recorded data number	$N = 100$
Internal states boundary	$\boldsymbol{\eta}_{\min} = [-\pi/3, -1]^T$, $\boldsymbol{\eta}_{\max} = [\pi/3, 1]^T$

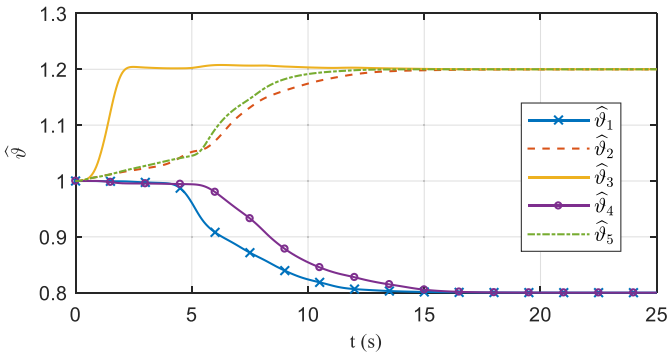

Fig. 5. Parameter estimation.

The initial conditions are

$$\begin{aligned}&\boldsymbol{x} = \boldsymbol{0}, \ \ \boldsymbol{h}_{\boldsymbol{x}} = \boldsymbol{h}_z = \boldsymbol{h}_\theta = \boldsymbol{0}, \ \ l_{\boldsymbol{x}} = l_z = l_\theta = 0 \\ &\hat{\boldsymbol{\vartheta}}_{\boldsymbol{x}} = \left[\hat{\vartheta}_1, \hat{\vartheta}_2\right]^T = [1, 1]^T, \ \ \hat{\boldsymbol{\vartheta}}_z = \left[\hat{\vartheta}_3, \hat{\vartheta}_4\right]^T = [1, 1]^T \\ &\hat{\boldsymbol{\vartheta}}_\theta = \hat{\vartheta}_5 = 1. \end{aligned}$$

The controller parameters are given in Table I.

The simulation results are shown in Figs. 5 and 6. From Fig. 5, it can be observed that all the identified parameters converge to their true values quickly, which verifies that the experience replay technique can achieve an excellent identification for the uncertain parameters. From Fig. 6, it can be observed that both outputs x and z converge to their references quickly. After 15 s, the parameter estimations nearly approach their true values and the outputs almost coincide with the references. In addition, the internal state θ also converges to the IID quickly which indicates the internal dynamics are well stabilized.

For further investigation on the performance of the proposed method, a comparison is made between the proposed method and traditional stable inversion [11] method without parameter identification. Three cases are considered, where the IID are calculated by different methods and are incorporated into the same controller (6). Case 1 uses the proposed method to obtain the IID, case 2 uses stable inversion with the nominal parameters, and case 3 uses stable inversion with the true parameters. The tracking error $e_x = x - x_r$ is shown in Fig. 7. On the one hand, it can be seen that the tracking error in

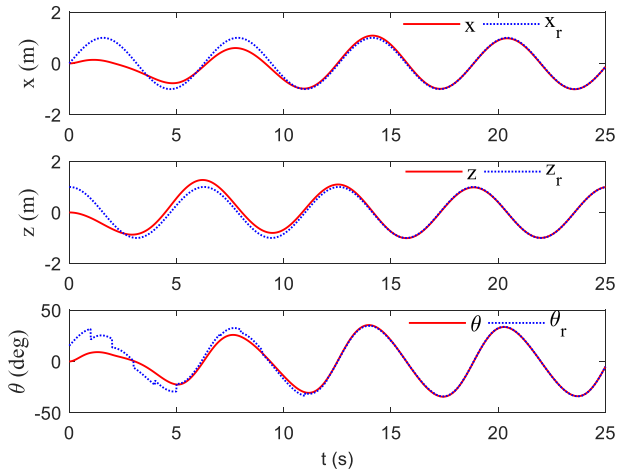

Fig. 6. Tracking curves of outputs and internal state.

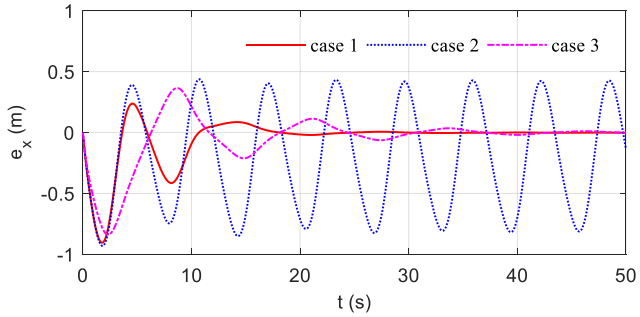

Fig. 7. Tracking error for different methods. Case 1: Proposed method. Case 2: Stable inversion with nominal parameters. Case 3: Stable inversion with true parameters.

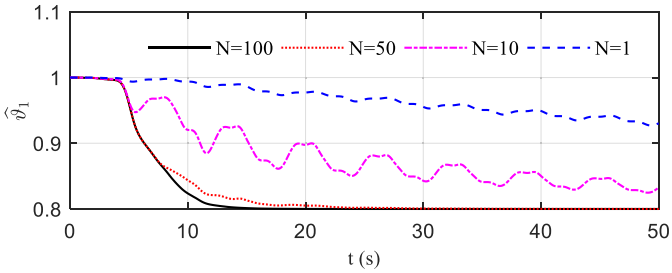

Fig. 8. Identification result with different recorded data numbers.

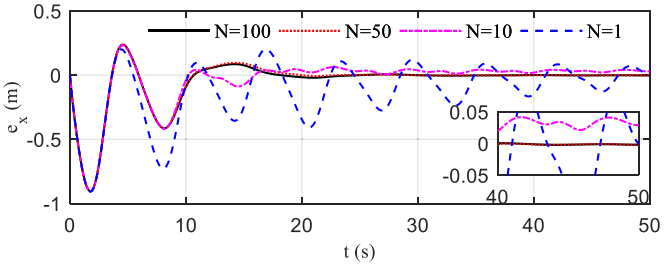

Fig. 9. Tracking error with different recorded data numbers.

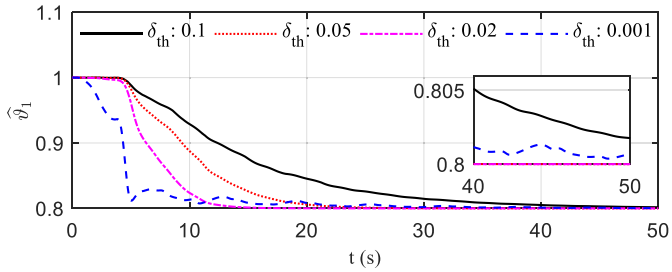

Fig. 10. Identification result with different data collection thresholds.

case 2 does not converge, which indicates that traditional stable inversion will result in tracking error if the parameters are deviated from their nominal values. On the other hand, the tracking error in cases 1 and 3 can converge to nearly zero, where case 1 converges faster. This verifies the effectiveness of the proposed method. Since optimal bounded inversion can minimize the initial condition mismatch of the internal states, the transient tracking performance is improved.

B. Further Results

The experience replay technique plays an important role in the proposed method. It is found that the recorded data number N and the data collection threshold δ_{th} have great influence on the identification and tracking performance. To evaluate their impacts, some qualitative and quantitative analyses are made.

1) Impact of Recorded Data Number: To explore the impact of the recorded data number, a comparison is made with different recorded data number. The identification result is shown in Fig. 8 and the tracking error is shown in Fig. 9.

It can be seen that the recorded data number is crucial for identification and output tracking. The identification and tracking performance are better with more recorded data. When the recorded data number $N = 1$, it means that only the current data is used, thus the experience replay algorithm degrades into traditional adaptive algorithm, where the identification and tracking performance are very bad. When the recorded data number is big enough (say 100 in this example), the identification can hardly be improved, and it does not limit the tracking performance any more. In real applications, a proper data collection number should be specified to ensure a good performance and match the hardware's storage capacity as well.

2) Impact of Data Collection Threshold: To explore the impact of the data collection threshold, a comparison is made with different data collection threshold. The identification result is shown in Fig. 10 and the tracking error is shown in Fig. 11. It can be seen that the data collection threshold has a significant effect on the identification and tracking performance. On the one hand, when the data collection threshold is big (say 0.1), the identification converges slowly, and the transient tracking performance is not so good. On the other hand, when the data collection threshold is too small (say 0.001), the identification will not converge and there is a steady-state tracking error. In real applications, a proper data collection threshold should be specified to balance the transient tracking performance and the steady-state tracking error.

Based on the analyses above, the impacts of the two data collection parameters are summarized in Table II.

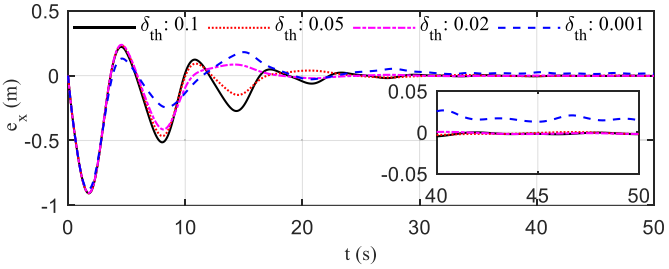

Fig. 11. Tracking error with different data collection thresholds.

TABLE II
IMPACTS OF DATA COLLECTION PARAMETERS

Parameters	Too small	Too big
Recorded data number (N)	Steady-state tracking error	More storage space
Data collection threshold (δ_{th})	Steady-state tracking error	Bad transient tracking performance

According to Table II, the two parameters should be chosen properly. Generally speaking, the recorded data number should be chosen big enough to guarantee small steady-state tracking error. But too many recorded data will put higher demands on the system storage and is not necessary either since the recorded data number does not limit the tracking performance after it exceeds a certain bound (about 100 in this example). As for the data collection threshold, it should be chosen not too small and not too large to balance the transient tracking performance and the steady-state tracking error (0.02–0.05 seems proper in this example).

VI. CONCLUSION

This paper focuses on the IID calculation for the uncertain zero dynamics, which is the key to achieving precision output tracking for uncertain nonminimum phase systems. The experience replay technique is applied to identify the uncertain parameters, which makes use of the recorded data and can achieve fast convergence to the true value. Then, a new method called *optimal bounded inversion* is proposed for the IID calculation by using the powerful optimization tool GPOPS-II, which is easy to implement and has high efficiency as well as high accuracy. And a piecewise IID updating scheme is adopted to reduce the computational burden. The proposed method is very effective for precision output tracking of MIMO nonlinear nonminmum phase systems with uncertain parameters as verified by the VTOL example. Future work will focus on enhancing the robust stability of the controller.

REFERENCES

[1] A. Isidori, *Nonlinear Control Systems*. London, U.K.: Springer, 2013.
[2] L. Ye, Q. Zong, J. L. Crassidis, and B. Tian, "Output-redefinition-based dynamic inversion control for a nonminimum phase hypersonic vehicle," *IEEE Trans. Ind. Electron.*, vol. 65, no. 4, pp. 3447–3457, Apr. 2018.
[3] Z. Wang, W. Bao, and H. Li, "Second-order dynamic sliding-mode control for nonminimum phase underactuated hypersonic vehicles," *IEEE Trans. Ind. Electron.*, vol. 64, no. 4, pp. 3105–3112, Apr. 2017.
[4] W. Lin, W. Wei, and G. Ye, "Global stabilization of a class of nonminimum-phase nonlinear systems by sampled-data output feedback," *IEEE Trans. Autom. Control*, vol. 61, no. 10, pp. 3076–3082, Oct. 2016.
[5] S. Gopalswamy and J. K. Hedrick, "Tracking nonlinear non-minimum phase systems using sliding control," *Int. J. Control*, vol. 57, no. 5, pp. 1141–1158, 1993.
[6] J. Huang, *Nonlinear Output Regulation: Theory and Applications*. Philadelphia, PA, USA: SIAM, 2004.
[7] Y. Ji, H. Zhou, and Q. Zong, "Approximate output regulation of non-minimum phase hypersonic flight vehicle," *Nonlin. Dyn.*, vol. 91, no. 4, pp. 2715–2724, 2018.
[8] I. A. Shkolnikov and Y. B. Shtessel, "Tracking controller design for a class of nonminimum-phase systems via the method of system center," *IEEE Trans. Autom. Control*, vol. 46, no. 10, pp. 1639–1643, Oct. 2001.
[9] I. A. Shkolnikov and Y. B. Shtessel, "Tracking in a class of nonminimum-phase systems with nonlinear internal dynamics via sliding mode control using method of system center," *Automatica*, vol. 38, no. 5, pp. 837–842, 2002.
[10] L. Postelnik, A. K. Swain, and K. A. Stol, "Approximate stable system centre approach to output tracking of non-minimum phase nonlinear systems," *J. Frankl. Inst.*, vol. 354, no. 8 pp. 3322–3340, 2017.
[11] S. Devasia, D. Chen, and B. Paden, "Nonlinear inversion-based output tracking," *IEEE Trans. Autom. Control*, vol. 41, no. 7, pp. 930–942, Jul. 1996.
[12] L. R. Hunt and G. Meyer, "Stable inversion for nonlinear systems," *Automatica*, vol. 33, no. 8, pp. 1549–1554, 1997.
[13] Y. Zhang, Q. Zhu, and R. Xiong, "Precise tracking for continuous-time non-minimum phase systems," *Asian J. Control*, Sep. 2018. doi: 10.1002/asjc.1866.
[14] D. G. Taylor and S. Li, "Stable inversion of continuous-time nonlinear systems by finite-difference methods," *IEEE Trans. Autom. Control*, vol. 47, no. 3, pp. 537–542, Mar. 2002.
[15] T. Sogo, "On the equivalence between stable inversion for nonminimum phase systems and reciprocal transfer functions defined by the two-sided Laplace transform," *Automatica*, vol. 46, no. 1, pp. 122–126, 2010.
[16] K. Graichen, V. Hagenmeyer, and M. Zeitz, "A new approach to inversion-based feedforward control design for nonlinear systems," *Automatica*, vol. 41, no.12, pp. 2033–2041, 2005.
[17] O. Brüls, G. J. Bastos, and R. Seifried, "A stable inversion method for feedforward control of constrained flexible multibody systems," *J. Comput. Nonlin. Dyn.*, vol. 9, no. 1, 2014, Art. no. 011014.
[18] Q. Zou and S. Devasia, "Precision preview-based stable-inversion for nonlinear nonminimum-phase systems: The VTOL example," *Automatica*, vol. 43, no. 1, pp. 117–127, 2007.
[19] Q. Zou, "Optimal preview-based stable-inversion for output tracking of nonminimum-phase linear systems," *Automatica*, vol. 45, no. 1, pp. 230–237, 2009.
[20] A. Boekfah, and S. Devasia, "Output-boundary regulation using event-based feedforward for nonminimum-phase systems," *IEEE Trans. Control Syst. Technol.*, vol. 24, no. 1, pp. 265–275, Jan. 2016.
[21] X. Hu, Y. Zhao, B. Xu, and C. Hu, "Robust adaptive fuzzy tracking control for uncertain MIMO nonlinear nonminimum phase system," *IEEE Trans. Syst., Man, Cybern., Syst.*, to be published. doi: 10.1109/TSMC.2018.2792139.
[22] X. Hu, C. Hu, X. Si, and Y. Zhao, "Robust sliding mode-based learning control for MIMO nonlinear nonminimum phase system in general form," *IEEE Trans. Cybern.*, to be published. doi: 10.1109/TCYB.2018.2874682.
[23] H. Modares, F. L. Lewis, and M.-B. Naghibi-Sistani, "Adaptive optimal control of unknown constrained-input systems using policy iteration and neural networks," *IEEE Trans. Neural Netw. Learn. Syst.*, vol. 24, no. 10, pp. 1513–1525, Oct. 2013.
[24] H. Modares, F. L. Lewis, and M. B. Naghibi-Sistani, "Integral reinforcement learning and experience replay for adaptive optimal control of partially-unknown constrained-input continuous-time systems," *Automatica*, vol. 50, no. 1, pp. 193–202, 2014.
[25] M. A. Patterson and A. V. Rao, "GPOPS-II: A MATLAB software for solving multiple-phase optimal control problems using hp-adaptive Gaussian quadrature collocation methods and sparse nonlinear programming," *ACM Trans. Math. Softw.*, vol. 41, no. 1, pp. 1–37, 2014.
[26] M. Chen and S. S. Ge, "Adaptive neural output feedback control of uncertain nonlinear systems with unknown hysteresis using disturbance observer," *IEEE Trans. Ind. Electron.*, vol. 62, no. 12, pp. 7706–7716, Dec. 2015.

[27] M. Chen, P. Shi, and C.-C. Lim, "Adaptive neural fault-tolerant control of a 3-DOF model helicopter system," *IEEE Trans. Syst., Man, Cybern., Syst.*, vol. 46, no. 2, pp. 260–270, Feb. 2016.
[28] M. Chen, S.-Y. Shao, and B. Jiang, "Adaptive neural control of uncertain nonlinear systems using disturbance observer," *IEEE Trans. Cybern.*, vol. 47, no. 10, pp. 3110–3123, Oct. 2017.
[29] S. Nazrulla and H. K. Khalil, "Robust stabilization of non-minimum phase nonlinear systems using extended high-gain observers," *IEEE Trans. Autom. Control*, vol. 56, no. 4, pp. 802–813, Apr. 2011.
[30] W. Lin and W. Wei, "Robust control of a family of uncertain nonminimum-phase systems via continuous-time and sampled-data output feedback," *Int. J. Robust Nonlin. Control*, vol. 28, no. 4, pp. 1440–1455, 2018.
[31] G. Tao, *Adaptive Control Design and Analysis*. Hoboken, NJ, USA: Wiley, 2003.
[32] G. Teschl, *Ordinary Differential Equations and Dynamical Systems*. Providence, RI, USA: Amer. Math. Soc., 2012.

Linqi Ye received the bachelor's degree in automation from Tianjin University, Tianjin, China, in 2014, where he is currently pursuing the Ph.D. degree in control science and engineering with the School of Electrical and Information Engineering.

He will be a Post-Doctoral Researcher with Tsinghua University, Beijing, China. From 2017 to 2018, he was a Visiting Scientist with the Sibley School of Mechanical and Aerospace Engineering, Cornell University, Ithaca, NY, USA. From 2016 to 2017, he was a Visiting Scholar with the Department of Mechanical and Aerospace Engineering, State University of New York at Buffalo, Buffalo, NY, USA. His current research interests include control of aerospace and robotic systems.

Qun Zong (M'04) received the bachelor's, master's, and Ph.D. degrees in automatic control from Tianjin University, Tianjin, China, in 1983, 1988, and 2002, respectively.

He is currently a Professor with the School of Electrical and Information Engineering, Tianjin University. His current research interests include complex system modeling and flight control.

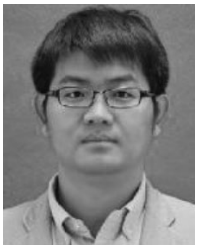

Bailing Tian (M'11) received the B.S., M.S., and Ph.D. degrees in automatic control from Tianjin University, Tianjin, China, in 2006, 2008, and 2011, respectively.

He was an Academic Visitor with the School of Electrical and Electronic Engineering, University of Manchester, Manchester, U.K., from 2014 to 2015. He is currently a Distinguished Research Fellow with the School of Electrical and Information Engineering, Tianjin University. His current research interests include finite-time control and integrated guidance and control for vehicle.